Batteries & Supercaps

Research Article
doi.org/10.1002/batt.202500484

Chemistry Europe
European Chemical Societies Publishing

www.batteries-supercaps.org

Effect of Side-Chain Modifications on Salt-Concentrated Poly(Ionic Liquid) Electrolytes

Kewei Cai, Jhonatan Soto Puelles, Shinji Kondou, Sreehari Batni Ravindranath, Maria Forsyth, and Fangfang Chen*

Poly(ionic liquid)-in-salt (PolyIL-in-salt) systems offer a promising pathway towards next-generation, safe, and high-performance all-solid-state alkali metal batteries. This study investigates the effect of side-chain modifications on ion transport in both neat and salt-containing polymer systems based on polydiallyldimethylammonium bistriflimide. Three types of side chains, i.e., methoxyethane, butyl, and isobutyl chains, were introduced to replace one methyl group to evaluate the influences of functional group, side-chain length, and branching. All modified polymers exhibit decreased glass transition temperature and increased anion diffusion in the neat state, which can be associated with weakened polycation-anion interaction. In salt-concentrated systems, ion diffusion varied between lithium and sodium systems, with a possible correlation to the change in free volume. Notably, the methoxyethane-substituted system shows the highest ionic diffusivity for both salts. This work provides valuable insights for the rational design of PolyIL-in-salt electrolytes with enhanced ionic conductivity.

1. Introduction

Solid polymer electrolytes (SPE) have attracted great interest in recent years for the development of solid-state batteries, particularly for electrical vehicle (EV) applications, due to their advantages in safety, mechanical integrity, and flexibility. However, significant challenges still hinder the widespread commercialization of SPEs, including low metal ion conductivity and transference number. The ion transference number represents the fraction of the total ionic conductivities contributed by metal cations. A low transference number arises from the significantly faster movement of anions compared to charge-carrying metal ions, which may be improved by increasing charge-carrier ion concentrations, but often at the cost of reduced ionic conductivity.

Poly(ionic liquids) (PolyILs), as a class of novel functional materials, have been used in a wide range of interdisciplinary applications, including but not limited to catalysis, separation, sensing, and electrolytes.[1] Our recent research highlights the great potential of cationic PolyILs as polymer electrolytes in obtaining both high conductivity and high metal ion transference numbers.[2] These materials offer suitable dielectric constants for metal-ion salt dissociation while exhibiting excellent chemical compatibility and electrochemical stability. Since the cations are tethered to the polymer backbone,[3] anion movement is significantly restricted, facilitating higher metal ion diffusion. Furthermore, the increased conductivities were observed at elevated salt concentrations, making PolyILs excellent candidates for developing salt-concentrated polymer electrolytes, benefiting an extended electrochemical stability window.

Promising results have been demonstrated in a PolyIL, polydiallyldimethylammonium fluorosulfonylimide (PDADMA FSI), with lithium (Li), sodium (Na) and potassium (K) salts. A conductivity of 0.7×10^{-4} S cm^{-1} and a $T_{Li} > 0.5$ was obtained at 80 °C for PDADMA FSI with LiFSI at a 1:1.5 molar ratio.[2a] Even faster Na transport was obtained for a 1:2 PDADMA FSI:NaFSI system, yielding a conductivity approaching 10^{-3} S cm^{-1} and a T_{Na} of around 0.57 at 80 °C.[2b] These promising results inspire further exploration and design of novel PolyILs with enhanced properties essential for their practical applications.

The ionic conductivity of PEs is affected by their chemical structure, composition, and physical properties and is closely associated with the polymer's glass transition temperature (T_g). A higher T_g restricts polymer segmental motion,[3,4] which inversely affects metal ion movement when their motion is coupled. This relationship has also been observed in PolyILs. Consequently, reducing the T_g of PolyILs is an effective way to enhance molecular mobility and improve ionic conductivity.[5]

Factors such as side chain length, chain rigidity, and counterion have been found to affect the T_g of PolyILs in previous research.[6] For instance, increasing the side chain length (e.g., for the C_nH_{2n+1} alkyl chain) can lower the T_g by tens of degrees and increase ionic conductivity by several orders of magnitude,

K. Cai, J. S. Puelles, S. Kondou, S. B. Ravindranath, M. Forsyth, F. Chen
Institute for Frontier Materials
Deakin University
Burwood, VIC 3125, Australia
E-mail: Fangfang.chen@deakin.edu.au

S. Kondou
Department of Materials Engineering Science
Osaka University
1-3, Machikaneyama, Toyonaka, Osaka 560-8531, Japan

Supporting information for this article is available on the WWW under https://doi.org/10.1002/batt.202500484

Research Article
doi.org/10.1002/batt.202500484
Chemistry Europe
European Chemical Societies Publishing

but an opposite trend was observed for the T_g-scaled conductivity.[6b,6c,7] Additionally, the side-chain-induced reduction in T_g is less pronounced in salt-containing PolyIL.[6b]

Enhancing chain flexibility, such as through ether functionalization of the polycation side chains, has also been demonstrated to effectively lower T_g.[8] Additionally, the salt addition has led to a significant T_g reduction in certain PolyILs, such as PDADMA FSI and poly(vinyl-1-methylimidazolium) (PVyMIM) FSI, both of which contain shorter alkyl side chains.[2a,9] However, this T_g lowering effect is not observed in analogous imidazolium-based PolyILs with longer side chains.[6b] Conversely, in 1-alkyl-3-vinylimidazolium bistriflimide-derived homopolymers P(C_nVm-TFSI) with longer alkyl chains ($n = 4$–10), the addition of 25 mol% Li salt results in an increase in T_g, despite that conductivity still improves for systems with $n = 4$–6.[6b] The underlying mechanism remains unclear.

Notably, PDADMA has a unique polymer architecture in which the cationic charge center resides on the polymer backbone, unlike most PolyILs where the cationic group are positioned on the side chains. Therefore, it is of great interest to understand the role of side chains in PDADMA-based analogs. Moreover, the influence of side-chain structure in salt-containing PolyILs, particularly at high salt concentrations, remains largely unexplored, providing additional motivation for this study.

In this work, we examined effect of side chains through three PDADMA-based analogs (**Figure 1**a): poly(diallyl methylbutyl ammonium) (PN14), poly(diallyl methylisobutyl ammonium) (PN1i4), and poly(diallyl methoxyethyl ammonium) (PN1,2O1), with the TFSI anion. Ordriozola and coworkers previously reported T_g of PN14 TFSI (40.3 °C) and PN1,2O1 TFSI (18.2 °C),[10] which are significant lower than that of PDADMA TFSI (116 °C).[16] We first simulated the T_g of the four PolyILs using

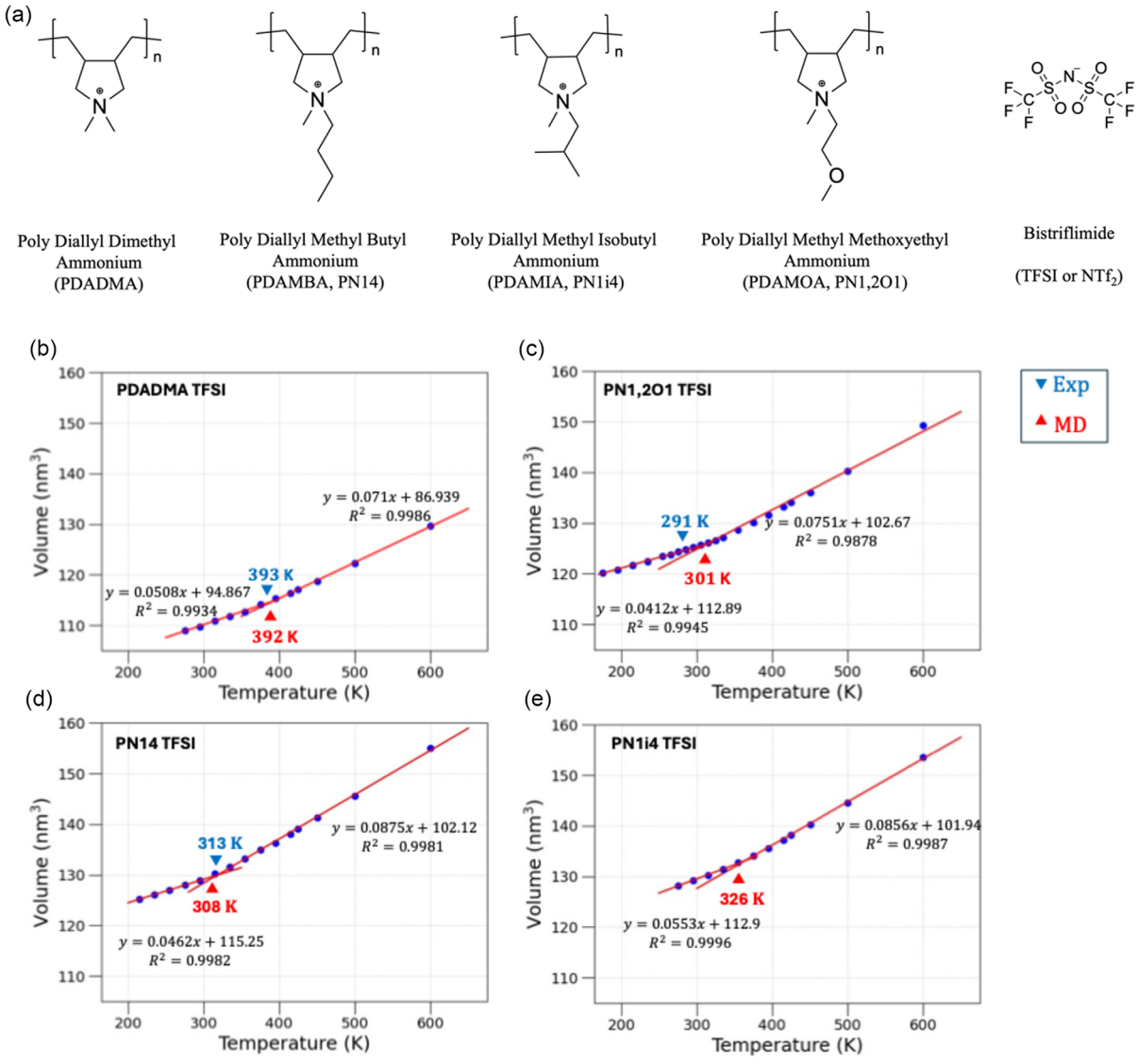

Figure 1. a) Chemical structures of four PolyILs and VT profiles from MD simulations for b) PDADMA TFSI, c) PN1,2O1 TFSI, d) PN14 TFSI, and e) PN1i4 TFSI. The experimental and simulated T_g are marked with the linear regression fitting and coefficient of determination R^2 provided.

molecular dynamics (MD) simulations and compared the results with experimental data. We then investigated the polycation-anion interaction by density functional theory (DFT), revealing a trend that correlate with T_g, and TFSI diffusion. Next, we extended the investigation to salt concentrated PolyIL systems with a 1:2 PolyIL to Li (Na) salt molar ratio and analyzed ion diffusion behavior. Our results show that while increasing the side chain length enhances anion diffusion in the three investigated PolyILs in their pure states in comparison with the PDADMA TFSI, only the PN1,2O1 TFSI system presents higher ion diffusion in the PolyIL-in-salt materials with both LiTFSI and NaTFSI salts. The PDADMA TFSI still presents the second most diffusive system with the Na salt but becomes the least diffusive system with the Li salt. Notably, the ion diffusivity order correlates with the order of volume expansion observed upon salt addition in the high-concentrated regime (polycation:salt = 1:2). This suggests that increased free volume may contribute to enhanced ion diffusion in salt-concentrated PolyILs. Further investigation is needed to confirm whether this trend holds at lower salt concentrations.

2. Computational Methodology

2.1. Force Field

The all-atom OPLS-AA force field was adopted for polycations, and the parameters were generated for the oligomer using the OPLS-AA online generator LigParGen.[11] It is important to note that monomer structures differentiated by torsion angles (i.e., different structural minima) can affect the generated parameters. We selected a set of parameters (Supplementary Information) that are consistent with those previously used and validated for PDADMA.[2a] In this set of parameters, the cation nitrogen atom carries a small and sometimes negative charge, which differs from the large positive charge for the nitrogen in ammonium cations when simulating ionic liquids. The parameters of Li and Na ions and TFSI anions were taken from the CL&P force field developed by Canongia Lopes and Padua, who adopted the same OPLS-AA functional form for this force field.[12] The charge was scaled down by a scale factor of 0.7 to account for the polarizable effect.

2.2. Simulation Box

A single polymer chain consisting of 20 polycation repeat units (Degree of Polymerization, DP = 20) was generated using Avogadro 1.0 software. The single polymer chain was optimized with the Merck molecular force field 94 (MMFF94).[13] For the PolyIL system, the simulation box contains 12 polymer chains and 240 TFSI anions. For the PolyIL/salt system, an additional 480 Li-TFSI or Na-TFSI ion pairs were introduced, giving a PolyIL to salt ratio of 1:2. The simulation box and the force field files were constructed using fftool[12] and Packmol.[14]

2.3. MD Simulation Details

All MD simulations were performed using the GROMACS 2022 software package.[15] Initial energy minimization was performed using the steepest descent algorithm with a convergence tolerance of 1000 kJ mol^{-1} nm^{-1}, defined as the maximum force acting on any atom. This was carried out using the standard GROMACS energy minimization routine. To better equilibrate the polymer electrolyte systems, we employed the "21-step equilibrium method" (Table S1, Supporting Information), developed by Colina and coworkers based on Hofmann's protocol.[16] It is important to note that ion diffusion in PEs is highly sensitive to the structural equilibration process. The traditional annealing procedure, which involves heating and stepwise cooling processes, could be inadequately to deal with rigid and porous polymer systems with sluggish dynamics. As a result, it may fail in removing heterogeneous free volumes exist in the initial randomly packed configuration, therefore, affects ion transport calculations and reproducibility. The "21-step equilibrium method" integrates canonical (NVT) and isothermal–isobaric (NPT) simulations, employing both high temperature and high pressure to overcome the large energy barriers of polymers. The additional compression steps help eliminate unreasonable free volumes, thereby improving the reproducibility of the simulated properties.[17]

Following the 21-step equilibration (Table S1, Supporting Information), the system was further equilibrated at 353 K for 50 ns using the NPT ensemble. The leap-frog integrator (integrator = md) and a time step of 1 fs were adopted. Temperature was controlled using the Nosé–Hoover thermostat with a time constant (tau-t) of 1 ps. Pressure was maintained at 1 bar using the Parrinello–Rahman barostat with a coupling constant (tau-p) of 1.0 ps and a compressibility of 4.5×10^{-5} bar^{-1}. Long-range electrostatics were treated using the Particle Mesh Ewald (PME) method[18] with a real-space cutoff of 1.2 nm. Van der Waals interactions were also truncated at 1.2 nm, with long-range dispersion corrections applied to both energy and pressure.

Finally, a 100 ns NVT simulation was conducted to analyze ion diffusion behavior, which was maintained at 353 K using the Nosé–Hoover thermostat (tau-t = 1 ps). Long-range electrostatics were treated using the PME method with a real-space cutoff of 1.2 nm, a PME order of 4, and Fourier grid spacing of 0.16 nm. Van der Waals interactions were truncated at 1.2 nm, with long-range dispersion corrections applied to both energy and pressure. Periodic boundary conditions were applied in all three spatial dimensions. Bond constraints involving hydrogen atoms were enforced using the LINCS algorithm.[19]

The T_g of polymers is generally considered a "pseudo" second-order phase transition and is associated with a step change in heat capacity. It can be determined using differential scanning calorimetry (DSC) or through expansivity ($\alpha = dV/dT$), which can be experimentally measured experimentally via dilatometry. In molecular dynamics (MD) simulations, determining T_g via expansivity is straightforward. The volume–temperature (VT) relationship can be obtained through multiple NPT simulations.[17,20] In this approach, each polymer system was heated to 1000 K after

the "21 step equilibration" and then gradually cooled to 100 K in a stepwise manner. At each temperature step, the system was equilibrated for 50 ns in an NPT ensemble. The volume was plotted as a function of temperature, and T_g was determined by applying linear regression to the VT profile (Figure 1), which exhibited two distinct slopes. The intersection point of those slopes was identified as T_g. The accuracy and precision of the linear regression were assessed using the coefficient of determination (R^2), which should exceed 0.99, with 1 indicating a perfect fit. Please note that this method can sometimes predict T_g with large errors, with devidations of several tens of degrees from the experimental result. Here, we attempted to assess whether the method can at least reproduce the relative difference observed in experimental results.

The ion mean squared displacement (MSD) was generated using GROMACS from a 100 ns production NVT simulation at 353 K. The self-diffusion coefficient (D) was then estimated from the MSD profile using the following Equation (1)

$$D = \frac{1}{6}\lim_{t\to\infty}\frac{d}{dt} < |r(t) - r(0)|^2 > \quad (1)$$

The Li (or Na) transference number was estimated using D of Li (Na), TFSI and polycation unit and their molar number N based on Equation (2)

$$t_{Li} = \frac{N_{Li} \times D_{Li}}{N_{Li} \times D_{Li} + N_{TFSI} \times D_{TFSI} + N_{polycation} \times D_{polycation}} \quad (2)$$

2.4. DFT

DFT calculations were conducted using the Gaussian (G09) package.[21] The geometry optimization and frequency calculations were carried out using the Becke 3-parameter Lee-Yang-Parr (B3LYP) exchange-correlation functional with a 6-31 +G(d) basis set in the gas phase. The binding energy between the polycation and anion was calculated using Equation (3).

$$E_{binding} = E_{polycation-anion} - E_{polycation} - E_{anion} \quad (3)$$

The energy to remove a Na (Li)TFSI in a polycationTFSI-NaTFSI complex was calculated using Equation (4). E stands for the optimized conformational energy of each component and the whole complex.

$$E_{binding} = E_{complex} - E_{polycation\,TFSI} - E_{NaTFSI} \quad (4)$$

The orbital calculations followed the methodology of previous work[22] using Møller−Plesset second-order perturbation theory (MP2) with a 6-311+G(d,p) basis set in the gas phase.

3. Results and Discussion

3.1. Effect of Side Chains on Neat PolyILs

T_g of four PolyILs (Figure 1a) was studied through MD simulations of volume-temperature plots. The glass transition leads to a change in the slope of the VT profile (Figure 1b–e), and T_g is estimated at the intersection of two linear regression fitting lines, which have coefficients of determination R^2 larger than 0.99.

Promisingly, the predicted T_g of three PolyILs follows the order seen in experimental results,[10,23] with PDADMA TFSI having the highest T_g of 392 K. The lowest T_g is with PN1,2O1 TFSI (301 K), which contains a flexible methoxyethane chain, followed by PN14 TFSI (308 K) with a linear butyl chain, and the PN1i4 TFSI (326 K) with a branched isobutyl chain, highlighting the side-chain effect. Except for PN1i4 TFSI, for which experimental T_g was not found, the predicted T_g surprisingly shows very small deviations from experimental values (less than 10 K), with relative errors ranging from −0.25% to 3.4% (Table S2, Supporting Information). These results indicate that the adopted force field parameters can reasonably capture the relative differences in T_g across different PolyILs, supporting their use in studying salt-containing system later. However, we caution that this should not be taken as an evidence that MD can accurately predict absolute experimental T_g values, as the polymer systems used in our simulation have a much lower degree of polymerization (DP = 20) compared to experimental materials, which normally have DPs several hundred units higher.

The binding energy (E_b) was calculated between the polycation unit and anion using DFT (**Figure 2**a). A shorter side chain in the polycation is associated with a higher binding energy with the anion. The $|E_b|$ follows an order: PDADMA TFSI > PN1i4 TFSI > PN14 TFSI > PN1,2O1 TFSI. This decrease in binding energy with longer side chain could be due to several reasons. One is the steric hindrance from longer side chain which can hinder the close approach of anions. Furthermore, extended long side chains can partially shield the positive charge center, decreasing electrostatic interaction. The ether oxygen on side chain can shield the positive charge through dipole orientation and reduces the interaction between polycation and anion.

Clearly, a positive correlation is observed between $|E_b|$ and T_g in Figure 2b, where a lower $|E_b|$ is associated with a lower T_g. The MSD was calculated for nitrogen atoms for 50 ns at 353 K in both polycations and anions to investigate ion diffusion. Anion diffusion remains very similar among the three side-chain modified PolyILs, whereas it is much slower in PDADMA TFSI, which could be linked to its highest T_g.

The ion coordination structures were further studied by calculating the radial distribution function (RDF) of polycation–anion and polycation–polycation through their nitrogen atoms (**Figure 3**a,b). The coordination number (CN) was determined at the first RDF minimum (Table S3, Supporting Information). The polycation-anion RDFs show a primary peak spanning 4 to 10 Å, indicating an extended first coordination shell. Notably, PDADMA-TFSI has a slight narrower peak and a higher CN of 7.45 at a shorter cutoff distance of 9.48 Å, reflecting tighter ion pairing compared to PolyILs with longer side chains, whereas the PN14 and PN1,2O1 have a higher first coordination shell cutoff distance (≈9.6 Å) and a lower coordination number (6.6 and 6.8), reflecting the reduced coordinated anions due to spatial steric hindrance from longer side chains (Figure S1a–d, Supporting Information). Despite similar positions of the first RDF peaks

Research Article
doi.org/10.1002/batt.202500484
Chemistry Europe
European Chemical Societies Publishing

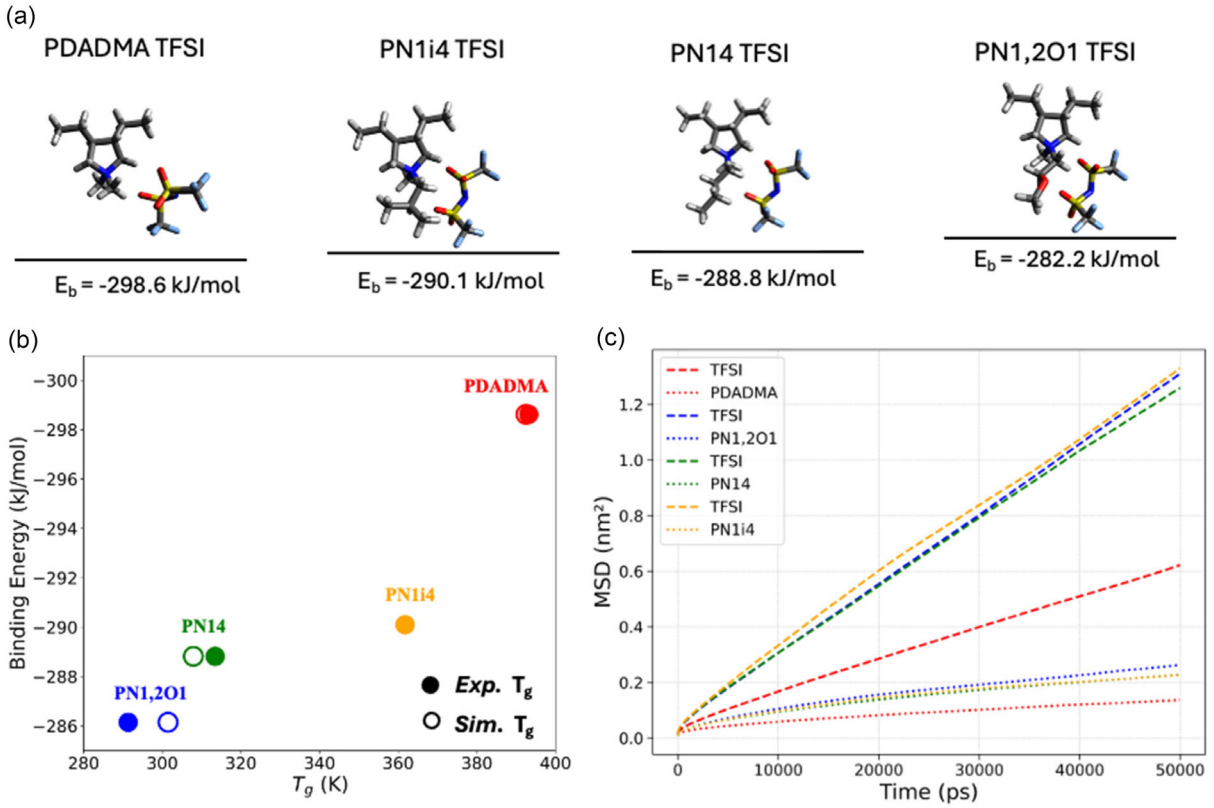

Figure 2. a) Optimized chemical structures of polycation units paired with TFSI anions. b) Binding energy (E_b) between polycations and anion against glass transition temperature (T_g). The solid and empty circles represent simulation and experimental data from literatures,[10,24] respectively. No experimental T_g is found for PN111i4. Color code: PDADMA (blue), PN1114 (green), PN111i4 (orange), and PN1,2O1(red). c) MSD profiles from MD simulation for TFSI (anion) and polycation in the neat polymer system.

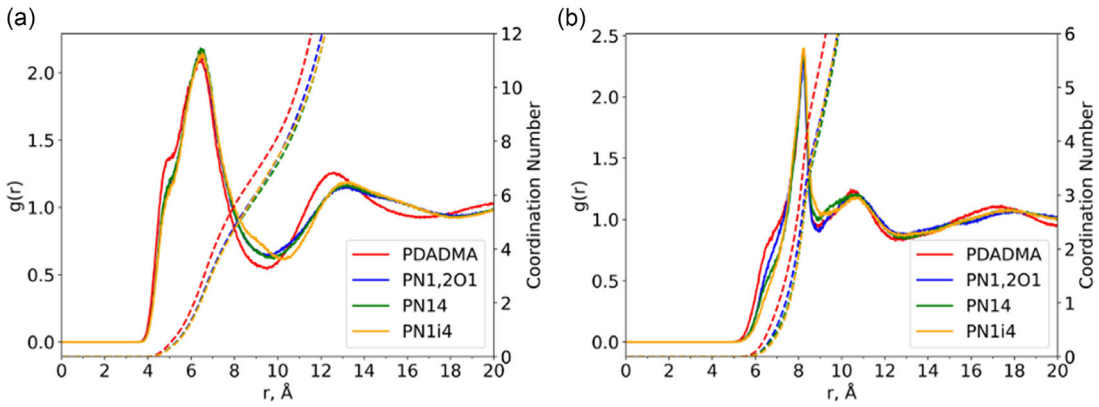

Figure 3. RDF and CN between a) polycation (N4) and TFSI (NBT) and b) polycation (N4) and polycation (N4).

across systems, the second RDF peak in PDADMA TFSI is closer (near 12 Å), further indicating a compact and structured ion coordination environment, which could be related to the slower ion motion in this system.

The polycation–polycation RDFs were also generated in Figure 3b. The prominent sharp peak at ≈8 Å arises from the arrangement of adjacent polycation units. A subtle shoulder near 6.5 Å is likely due to a relative closer and stronger crosslinking of two polycations through co-coordinating with the same anion. The two polycations could either be from the same polymer chain (adjacent or not, intrachain crosslinking) or different polymer chains (interchain crosslinking) (Figure S2, Supporting Information). Since interchain crosslinking can increase polymer chain rigidity while intrachain crosslinking may increase chain curvature and folding, we compared interchain and intrachain polycation-polycation RDFs in Figure S2, Supporting Information. However, we were only able to identify a relative lower degree of interchain crosslinking in PN1,2O1 at the cutoff of the first RDF shoulder peak.

Research Article
doi.org/10.1002/batt.202500484
Chemistry Europe
European Chemical Societies Publishing

This may be related to its lower T_g and higher TFSI diffusion. The difference in the RDFs between intrachain polycations is minor.

3.2. Effect of Side Chains on PolyIL-in-Salt Systems (Polycation:Salt = 1:2)

In this section, we investigate the effect of side chain modifications on metal cation diffusion in salt-concentrated PolyIL. Previous research has reported that a 1:2 PDADMA FSI to NaFSI ratio yields the highest conductivity.[2] Therefore, the same salt ratio is adopted in this work. The effect of salt concentration is beyond the scope of the present study. It is important to note that within our simulation timescale, both LiTFSI and NaTFSI salts are completely dissolved in the PolyILs without any crystallization. However, under experimental conditions, phase separation may occur due to either the solubility limitation of the salt or the formation of new phases which was previously observed,[2a] which can affect ion diffusion and conductivity. Nevertheless, our study focuses on providing a theoretical understanding of how side-chain structures affect ion transport in amorphous, salt-concentrated PolyILs.

Figure 4 investigates the Li or Na and polycation coordination environment through Li(Na)-TFSI and polycation-TFSI coordination structures through RDF. The first major Li(Na)-TFSI RDF peak consists of three distinct subpeaks, corresponding to different coordination geometries with TFSI through nitrogen atoms (A1), oxygen atoms in a bidentate way (A2), or in a monodentate way (A3). Polycations with longer side chains lead to a minor decrease in Li(Na)-TFSI coordination number compared to the PDADMA system, with CN decreasing from 5 to 4.9 for the Na salt system and from 4.3 to 4.1 for the Li salt system (Table S4, Supporting Information). A similar decrease in CN with longer side chains is also observed for polycation–anion (N4-NBT) coordination in Figure 4b,d and Table S5, Supporting Information, except for the PN1i4, due to a broader RDF peak, resulting in a higher CN, which is similar to the neat PolyIL system.

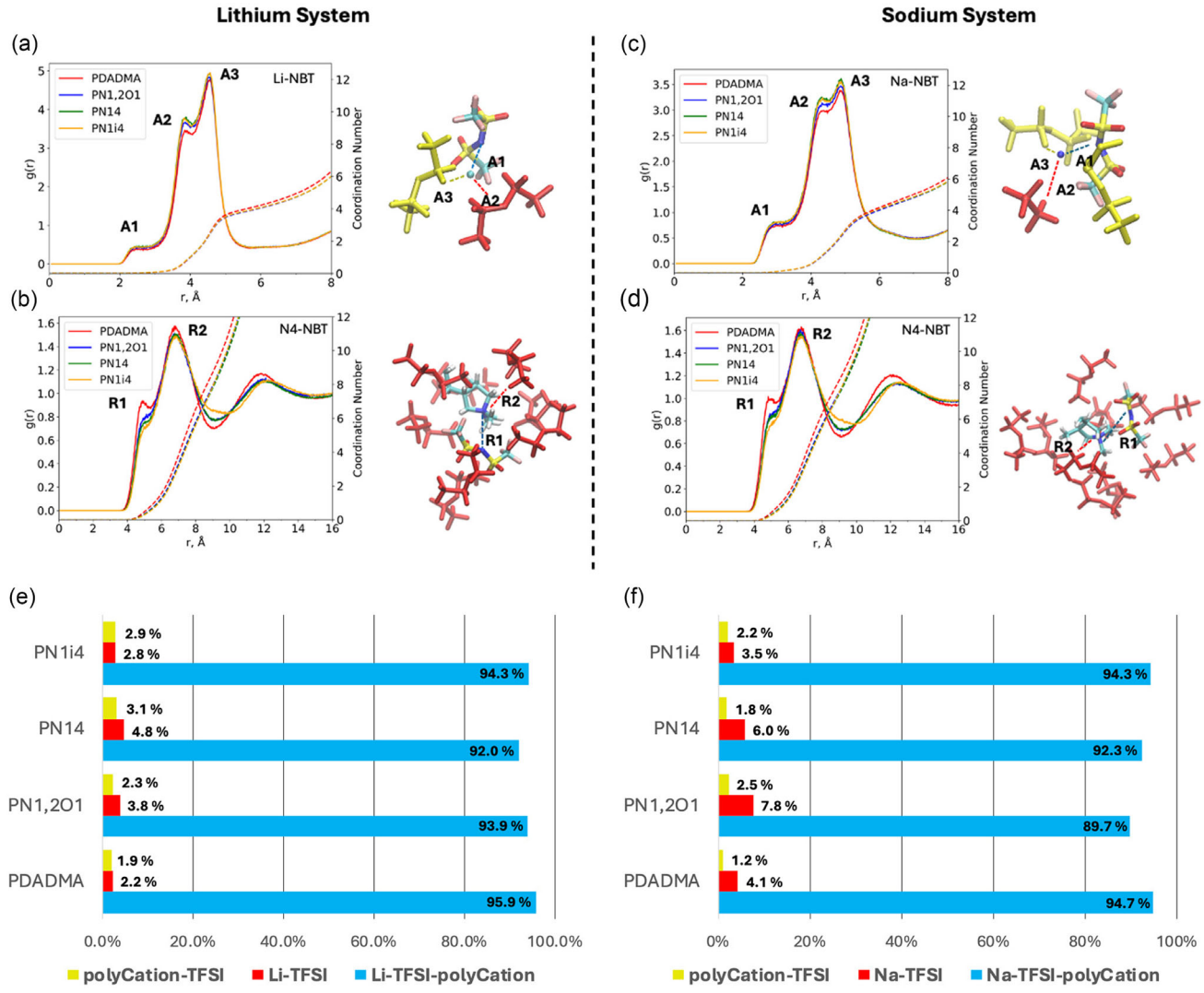

Figure 4. RDFs of a) Na-TFSI (NBT) and b) polycation (N4)-TFSI (NBT) in the Na system and c) Li-TFSI and d) polycation (N4)-TFSI (NBT) in the Li system. Percentages of anions in three types of coordination structures are analyzed for both e) Li salt and f) Na salt systems.

Research Article
doi.org/10.1002/batt.202500484
Chemistry Europe
European Chemical Societies Publishing

Three TFSI coordination states were analyzed in Figure 4e,f, which are TFSI coordinated with both polycations and metal ions (blue bar), with metal ions only (red bar), and with polycations only (yellow bar). Around 90% or more TFSI are in a co-coordination state, i.e., polycation-TFSI-Li (Na) coordination, suggesting that the salt is well dispersed throughout polymer matrix. This is further supported by the simulation snapshots shown in Figure S4, Supporting Information. The PDADMA system shows the highest co-coordination percentage, which is consistent with its higher polycation–anion and Li(Na)-anion CNs. When the polycation–anion coordination number decreases with longer side chains, the percentage of TFSI in the co-coordination state also decreases, and the percentage of TFSI coordinating with only Li or Na increases, potentially contributing to the formation of salt aggregates or molten salt state. However, this specific coordination state only accounts for less than 5% of TFSI in the Li system, and ≈3%–8% of TFSI in the Na system. Excess salt could have a double-side effect on conductivity, either enhancing or reducing it, depending on multifactors such as changes in T_g and the formation of a second phase. Our recent work has explored the impact of salt concentration, ranging from low to extremely high levels, in PolyILs, providing further insights.[20]

The diffusion of ions was investigated at 353 K by calculating their MSDs for over 50 ns from a 100 ns trajectory (**Figure 5**a,b). When comparing ion diffusivities across PolyILs, a consistent trend of PN1,2O1 > PN1i4 > PN14 was observed in both Li and Na systems. This order differs in the neat PolyILs where PN14 exhibits higher diffusion than PN1i4. Nevertheless, PN1,2O1 remains the most diffusive system in both neat and salt-containing PolyILs. In addition, the behavior of PDADMA differs between the Li and Na systems, and it is the second most diffusive in the Na systems but becomes the least diffusive in the Li salt systems.

This trend in diffusivities does not directly correlate with the coordination analysis but shows a strong correlation with the order of volume expansion in the PolyILs upon salt addition (Figure 5c,d and **Table 1**). Considering the same amount of salt added, the larger swelling may reflect an increase in free volume. Notably, PN1,2O1 TFSI exhibits the highest swelling with both Li

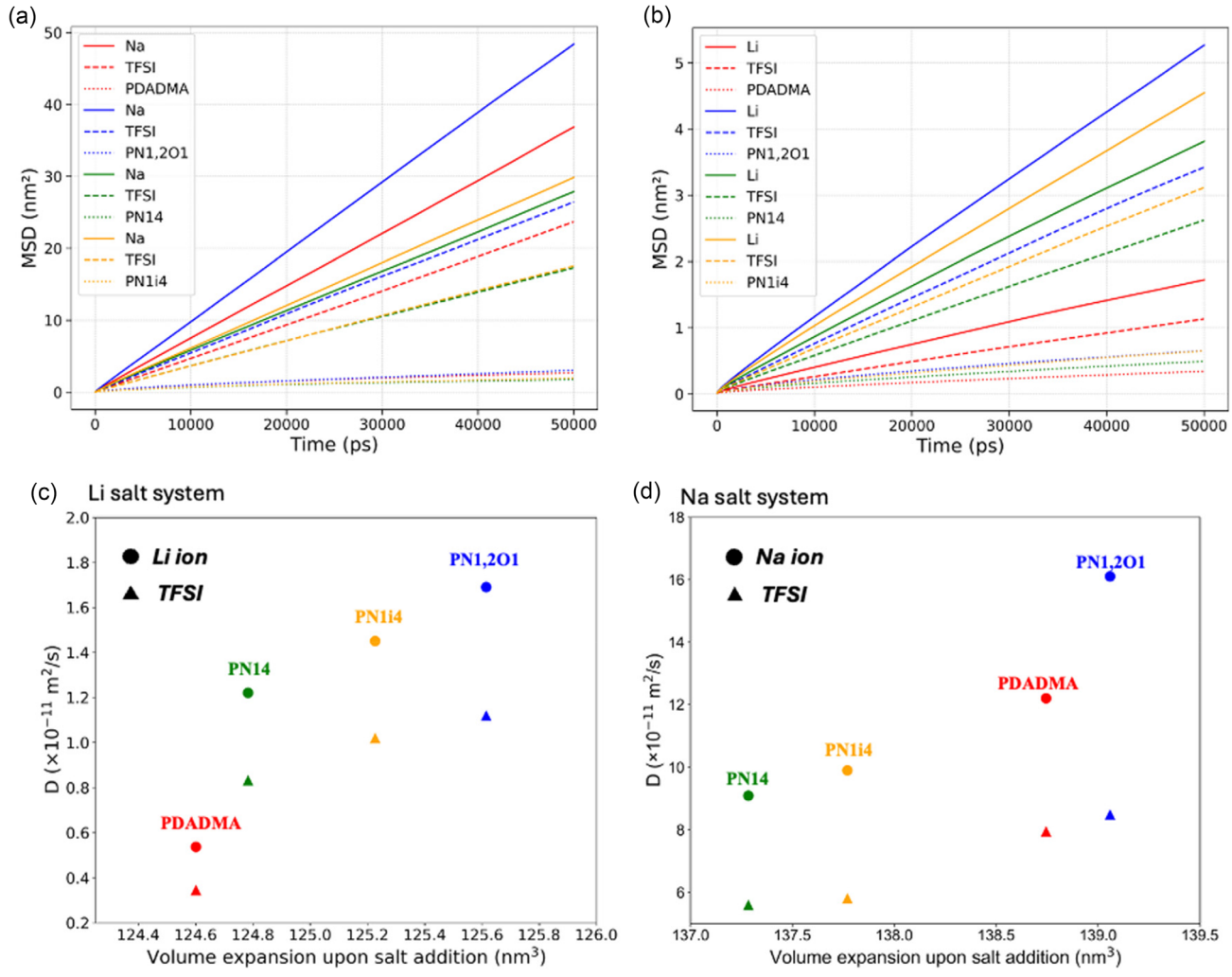

Figure 5. MSDs of Na (or Li),TFSI (through *N*) and polycation (through *N*) for PolyILs with a) NaTFSI and b) LiTFSI salt at 1:2 molar ratio and 353 K and the calculated Na (or Li) and TFSI self-diffusivities and the volume expansion upon adding salt for c) NaTFSI and d) LiTFSI systems.

Research Article
doi.org/10.1002/batt.202500484
Chemistry Europe
European Chemical Societies Publishing

Table 1. The equilibrated volume (nm^3) and error of the simulated box for neat PolyILs and their salt systems from NPT equilibration, with the volume changes after adding the salt.

	PolyIL	PolyIL + NaTFSI	ΔVolume	PolyIL + LiTFSI	ΔVolume
PDADMA	116.890 ± 0.010	255.659 ± 0.003	138.745 ± 0.013	241.517 ± 0.060	124.601± 0.070
PN14	141.045 ± 0.050	278.253 ± 0.076	137.284 ± 0.126	265.874 ± 0.048	124.783 ± 0.098
PN1i4	139.366 ± 0.025	277.134 ± 0.029	137.770 ± 0.054	264.568 ± 0.063	125.227 ± 0.088
PN1,2O1	136.426 ± 0.047	275.495 ± 0.018	139.059 ± 0.065	262.041 ± 0.020	125.615 ± 0.067

Table 2. Self-diffusion coefficients (10^{-11} m^2 s^{-1}) calculated for both Li and Na systems.

	D_{Li}	D_{TFSI}	$D_{polycation}$	D_{Li}/D_{TFSI}	T_{Li}
PDADMA	0.54 ± 0.04	0.35 ± 0.01	0.09 ± 0.00	1.54	0.49
PN1,2O1	1.69 ± 0.06	1.12 ± 0.12	0.16 ± 0.00	1.51	0.49
PN14	1.22 ± 0.04	0.83 ± 0.02	0.13 ± 0.03	1.47	0.48
PN1i4	1.45 ± 0.17	1.02 ± 0.04	0.20 ± 0.03	1.42	0.47
	D_{Na}	D_{TFSI}	$D_{polycation}$	D_{Na}/D_{TFSI}	T_{Na}	D_{Na}/D_{Li}
PDADMA	12.24 ± 0.44	7.95 ± 0.03	0.58 ± 0.04	1.54	0.50	22.7
PN1,2O1	16.12 ± 0.62	8.49 ± 0.34	0.81 ± 0.20	1.90	0.55	9.5
PN14	9.09 ± 0.42	5.60 ± 0.00	0.36 ± 0.20	1.62	0.51	7.5
PN1i4	9.90 ± 0.27	5.81 ± 0.02	0.42 ± 0.22	1.70	0.53	6.8

and Na salt, while PDADMA TFSI shows the second-highest swelling with NaTFSI and the least swelling with LiTFSI. The swelling of PN1i4 TFSI is higher than PN14 TFSI with both salts. These trends are happened to be associated with the observed order of ion diffusivities, indicating that free volume could play a key role in affecting ion diffusion in these super concentrated polymer electrolytes.

In addition, ion self-diffusion coefficients were calculated to estimate the Li and Na transport numbers (**Table 2**). For the Li salt systems, increasing the side chain length results in a slight decrease for D_{Li}/D_{TFSI} ratio, from 1.54 in PDADMA to 1.42 in PN1i4, accompanied by a reduction in Li transport number (T_{Li}) from 0.49 to 0.47. Overall, T_{Li} still remains close to 0.5, suggesting that side-chain modification can enhance Li conductivity and preserves a high Li transference number. For the Na systems, an increase in D_{Na}/D_{TFSI} ratio is observed for all side-chain modified systems due to a higher enhancement in Na diffusion, resulting in an increase in T_{Na}. Notably, the PN1,2O1 system shows both the highest ion diffusion enhancement and the highest T_{Na} of 0.55. Therefore, our modeling results suggest that replacing the methyl group with the methoxyethyl group as a side chain is an effective method in further enhancing electrolyte properties for both Li and Na salts added systems.

Moreover, when comparing the enhancement in metal ion diffusion in PN1,2O1 relative to PDADMA, i.e., the ratio of their D_{Li} or D_{Na} the side chain modification has a more pronounced effect for enhancing Li diffusion (3.1-fold increase) than for Na diffusion (1.3-fold). On the other hand, when comparing the D_{Na}/D_{Li} ratios across different PolyILs, PDADMA, which has shorter side chains, shows the highest ratio (22.7). This suggest that the difference in Li and Na diffusion tends to decrease with increasing side-chain size.

Overall, the PN1,2O1 TFSI holds great potential for improving metal ion diffusion at high salt concentrations compared to its PDADMA counterpart. Ether functionalization of side chains not only weaken polycation–anion interaction (E_b) but also leads to the highest volume expansion upon salt addition (Table 1). Both factors could co-contribute to its higher ion diffusion. Moreover, the ether oxygens in polycations can also provide additional coordination sites for Li and Na. We found that ≈6% of Li and 10% of Na ions have been coordinated with the ether oxygen in the polycation throughout the 100 ns MD trajectories through checking Li–O and Na–O distances. Importantly, this coordination is transient and does not hinder Li or Na diffusion, as indicated by the Li/Na–O pairing lifetimes between Li/Na–O(ether) and Li/Na–O(TFSI) in Figure S3, Supporting Information. In the Li system, the time correlation function of Li–O(ether) decays faster than that of Li–O(TFSI), reflecting the short-lived Li-polycation coordination. In the Na system, both profiles are very close and at faster decay rate compared to the Li system, reflecting the higher ion diffusivity. Therefore, we hypothesize that these additional short-lived Li/Na coordination sites increase the hoping pathways for metal ions, may further facilitating metal ion transport.

4. Conclusion

In this work, we conducted a computational investigation into the effect of side-chain modifications in polycations on ion diffusion in salt-concentrated PolyILs. Four polycations with different side chains—methyl, butyl, isobutyl, and methoxyethyl groups—were compared. Overall, longer side chains lowered

the glass transition temperature (T_g) of the PolyILs and weakened polycation–anion interactions, thereby enhancing anion diffusion. Side-chain modifications also induced variations in polymer morphology: longer side chains reduced interchain interactions and promoted intrachain folding. This may contribute to the observed decrease in T_g. Upon the addition of a high concentration of Li or Na salt, the same modified polycations exhibited different behaviors depending on the cation species, including differences in morphology and ion diffusivity. Ion diffusivities showed a strong correlation with the degree of volume expansion in the PolyILs upon salt addition. Notably, the PolyIL containing the ether-functionalized methoxyethyl group consistently demonstrated the highest performance among the four systems, underscoring the potential of side-chain engineering to enhance ion transport in salt-concentrated PolyILs. Additionally, a clear correlation was observed between the order of ion diffusivity and the order of volume expansion, highlighting the importance of increasing free volume to facilitate ion transport. This computational study provides valuable insights for the future design of PolyIL-based electrolytes for solid-state Li and Na batteries.

Acknowledgements

All authors acknowledge the Australian Research Council for financial support through the ARC Discovery Project (DP240101661). This research was undertaken with the assistance of resources from the National Computational Infrastructure (NCI Australia), an NCRIS-enabled capability supported by the Australian Government.

Open access publishing facilitated by Deakin University, as part of the Wiley - Deakin University agreement via the Council of Australian University Librarians.

Conflict of Interest

The authors declare no conflict of interest.

Data Availability Statement

The data that support the findings of this study are available from the corresponding author upon reasonable request.

Keywords: conductivity · molecular simulation · polymer electrolytes · solid-state metal batteries

[1] M. Zhu, Y. Yang, *Green Chem.* **2024**, *26*, 5022.
[2] a) X. Wang, F. Chen, G. M. Girard, H. Zhu, D. R. MacFarlane, D. Mecerreyes, M. Armand, P. C. Howlett, M. Forsyth, *Joule* **2019**, *3*, 2687; b) F. Chen, X. Wang, M. Armand, M. Forsyth, *Nat. Mater.* **2022**, *21*, 1175.
[3] D. Mecerreyes, *Prog. Polym. Sci.* **2011**, *36*, 1629.
[4] W. Qian, J. Texter, F. Yan, *Chem. Soc. Rev.* **2017**, *46*, 1124.
[5] D. Mecerreyes, N. Casado, I. Villaluenga, M. Forsyth, *Macromolecules* **2024**, *57*, 3013.
[6] a) D. S.-d. la Cruz, M. D. Green, Y. Ye, Y. A. Elabd, T. E. Long, K. I. Winey, J. Polym. *Sci., Part B: Polym. Phys.* **2012**, *50*, 338; b) V. Delhorbe, D. Bresser, H. Mendil-Jakani, P. Rannou, L. Bernard, T. Gutel, S. Lyonnard, L. Picard, *Macromolecules* **2017**, *50*, 4309; c) C. Iacob, A. Matsumoto, M. Brennan, H. Liu, S. J. Paddison, O. Urakawa, T. Inoue, J. Sangoro, J. Runt, *ACS Macro Lett.* **2017**, *6*, 941; d) M. D. Green, D. Salas-de la Cruz, Y. Ye, J. M. Layman, Y. A. Elabd, K. I. Winey, T. E. Long, *Macromol. Chem. Phys.* **2011**, *212*, 2522; e) Z. Zhang, J. Krajniak, J. R. Keith, V. Ganesan, *ACS Macro Lett.* **2019**, *8*, 1096; f) V. Bocharova, Z. Wojnarowska, P.-F. Cao, Y. Fu, R. Kumar, B. Li, V. N. Novikov, S. Zhao, A. Kisliuk, T. Saito, J. W. Mays, B. G. Sumpter, A. P. Sokolov, *J. Phys. Chem. B* **2017**, *121*, 11511.
[7] M. Heres, T. Cosby, E. U. Mapesa, H. Liu, S. Berdzinski, V. Strehmel, M. Dadmun, S. J. Paddison, J. Sangoro, *Macromolecules* **2019**, *52*, 88.
[8] H. Zhang, L. Li, W. Feng, Z. Zhou, J. Nie, *Polymer* **2014**, *55*, 3339.
[9] H. Zhang, W. Feng, Z. Zhou, J. Nie, *Solid State Ionics* **2014**, *256*, 61.
[10] M. Döbbelin, I. Azcune, M. Bedu, A. Ruiz de Luzuriaga, A. Genua, V. Jovanovski, G. Cabañero, I. Odriozola, *Chem. Mater.* **2012**, *24*, 1583.
[11] B. Doherty, X. Zhong, S. Gathiaka, B. Li, O. Acevedo, *J. Chem. Theory Comput.* **2017**, *13*, 6131.
[12] J. N. Canongia Lopes, A. A. H. Pádua, *Theor. Chem. Acc.* **2012**, *131*, 1129.
[13] M. D. Hanwell, D. E. Curtis, D. C. Lonie, T. Vandermeersch, E. Zurek, G. R. Hutchison, *J. Cheminform.* **2012**, *4*, 17.
[14] L. Martínez, R. Andrade, E. G. Birgin, J. M. Martínez, *J. Comput. Chem.* **2009**, *30*, 2157.
[15] D. Van Der Spoel, E. Lindahl, B. Hess, G. Groenhof, A. E. Mark, H. J. Berendsen, *J. Comput. Chem.* **2005**, *26*, 1701.
[16] D. Hofmann, L. Fritz, J. Ulbrich, C. Schepers, M. Böhning, *Macromol. Theory Simul.* **2000**, *9*, 293.
[17] L. J. Abbott, K. E. Hart, C. M. Colina, *Theor. Chem. Acc.* **2013**, *132*, 1334.
[18] U. Essmann, L. Perera, M. L. Berkowitz, T. Darden, H. Lee, L. G. Pedersen, *J. Chem. Phys.* **1995**, *103*, 8577.
[19] E. Krieger, G. Vriend, *J. Comput. Chem.* **2015**, *36*, 996.
[20] S. Kondou, M. Abdullah, I. Popov, M. L. Martins, L. A. O'Dell, H. Ueda, F. Makhlooghiazad, A. Nakanishi, T. Sudoh, K. Ueno, M. Watanabe, P. Howlett, H. Zhang, M. Armand, A. P. Sokolov, M. Forsyth, F. Chen, *J. Am. Chem. Soc.* **2024**, *146*, 33169.
[21] M. J. Frisch, G. W. Trucks, H. B. Schlegel, G. E. Scuseria, M. A. Robb, J. R. Cheeseman, G. Scalmani, V. Barone, G. A. Petersson, H. Nakatsuji, X. Li, M. Caricato, A. V. Marenich, J. Bloino, B. G. Janesko, R. Gomperts, B. Mennucci, H. P. Hratchian, J. V. Ortiz, A. F. Izmaylov, J. L. Sonnenberg, A. Williams, F. Ding, F. Lipparini, F. Egidi, J. Goings, B. Peng, A. Petrone, T. Henderson, D. Ranasinghe, et al., Wallingford, CT, **2016**.
[22] D. Rakov, M. Hasanpoor, A. Baskin, J. W. Lawson, F. Chen, P. V. Cherepanov, A. N. Simonov, P. C. Howlett, M. Forsyth, *Chem. Mater.* **2022**, *34*, 165.
[23] X. Wang, G. M. A. Girard, H. Zhu, R. Yunis, D. R. MacFarlane, D. Mecerreyes, A. J. Bhattacharyya, P. C. Howlett, M. Forsyth, *ACS Appl. Energy Mater.* **2019**, *2*, 6237.
[24] R. Yunis, G. M. A. Girard, X. Wang, H. Zhu, A. J. Bhattacharyya, P. Howlett, D. R. MacFarlane, M. Forsyth, *Solid State Ionics* **2018**, *327*, 83.

Manuscript received: June 26, 2025
Revised manuscript received: July 14, 2025
Version of record online: